

D. A. Wisniacki<sup>1</sup> and E. R. Pujals<sup>2</sup>

<sup>1</sup>*Departamento de Física “J. J. Giambiagi”, FCEN, UBA,  
Pabellón 1, Ciudad Universitaria, 1428 Buenos Aires, Argentina.*  
<sup>2</sup>*IMPA-OS, Dona Castorina 110, 22460-320 Rio de Janeiro, Brasil*

(Dated: January 28, 2005)

Bohmian mechanics is a causal interpretation of quantum mechanics in which particles describe trajectories guided by the wave function. The dynamics in the vicinity of nodes of the wave function, usually called vortices, is regular if they are at rest. However, vortices generically move during time evolution of the system. We show that this movement is the origin of chaotic behavior of quantum trajectories. As an example, our general result is numerically displayed in the two dimensional isotropic harmonic oscillator.

PACS numbers: PACS numbers: 05.45.-a, 03.65.-w

De Broglie-Bohm (BB) approach of quantum mechanics is experienced an increased popularity in nowadays. This is due to it combines the accuracy of the standard quantum description with the intuitive insight derived from the causal trajectory formalism, thus providing a powerful theoretical tool to understand the physical mechanisms underlying microscopic phenomena [1, 2]. Although the behavior of quantum trajectories are very different from classical solutions it can be used to gain intuition in many physical phenomena. Numerous examples can be found in different areas of research. In particular, we can mention studies of tunneling of smooth potential surfaces [3], the quantum back-reaction problem [4] or ballistic transport of electrons in nanowires [5].

According to BB theory of quantum motion, a particle moves in a deterministic orbit under the influence of the external potential and a quantum potential generated by the wave function. This quantum potential can be very intricate because it carry on wave interferences. Based on it, Bohm already predicted complex behavior of the quantum trajectories in his seminal work [6]. This was confirmed recently in several studies. These numerical works have shown the presence of chaos in various systems [7]. However, the mechanism that cause such a complex behavior is still lacking. In this letter we show that movement of the zeros of the wave function, called vortices in the literature, implies chaos in the dynamics of quantum trajectories. Such a movement perturb the velocity field producing transverse homoclinic orbits which generates the well known Small horseshoe, origin of complex behavior. Our assertion is based on an analytical proof in a simplified model which resembled the velocity field near vortices. Moreover, we present a numerical study in a 2-D isotropic harmonic oscillator that display a route to chaos dominated by this mechanism.

The fundamental equations in the BB theory are derived by introducing the wave function in polar form,  $\psi(\mathbf{r}, t) = R(\mathbf{r}, t) e^{iS(\mathbf{r}, t)}$  (throughout the paper  $\hbar$  is set equal to 1), into the time-dependent Schrödinger equation,

thus obtaining two real equations:

$$\frac{\partial R^2}{\partial t} + \nabla \cdot \left( R^2 \frac{\nabla S}{m} \right) = 0, \quad (1)$$

$$\frac{\partial S}{\partial t} + \frac{(\nabla S)^2}{2m} + V - \frac{1}{2m} \frac{\nabla^2 R}{R} = 0, \quad (2)$$

which are the continuity and quantum Hamilton–Jacobi equations, respectively. Here, the last term in the left–hand–side of Eq. (2) is the so–called quantum potential, a non–local function determined by the quantum state, which, together with  $V$ , determines the total force acting on the system. Similarly to what happens in the usual classical Hamilton–Jacobi theory, quantum trajectories of a particle of mass  $m$  can then be defined by means of the following velocity field equation:

$$\mathbf{v} = \dot{\mathbf{r}} = \frac{1}{m} \nabla S = \frac{i}{2m} \frac{\psi \nabla \psi^* - \psi^* \nabla \psi}{|\psi|^2}. \quad (3)$$

Vortices appear naturally in the BB framework. They result from wave function interferences so they have no classical explanation. In systems without magnetic field, the *bulk* vorticity  $\nabla \times \mathbf{v}$  in the probability fluid is determined by the points where the phase  $S$  is singular. This may occur only at points where the wave functions vanishes. This condition is fulfilled by isolated points in a 2-D system and lines in a 3-D system. Due to the single-valuedness of the wave function, the circulation  $\Gamma$  along any closed contour  $\xi$  encircling a vortex must be quantized, that is,

$$\Gamma = \int_{\xi} \dot{\mathbf{r}} d\mathbf{r} = \frac{2\pi n}{m}, \quad (4)$$

with  $n$  an integer [8, 9]. So, velocity  $\mathbf{v}$  must diverge as one approaches to a vortex. In fact, the time dependent velocity field in the vicinity of a vortex located at time  $t$  in  $\mathbf{r}_{\mathbf{v}}(t)$  is given by

$$\mathbf{v}_t = \frac{-i}{2m} \frac{[\mathbf{r} - \mathbf{r}_{\mathbf{v}}(t)] \times \mathbf{w} \times \mathbf{w}^*}{\left| [\mathbf{r} - \mathbf{r}_{\mathbf{v}}(t)] \cdot \mathbf{w} \right|^2}, \quad (5)$$

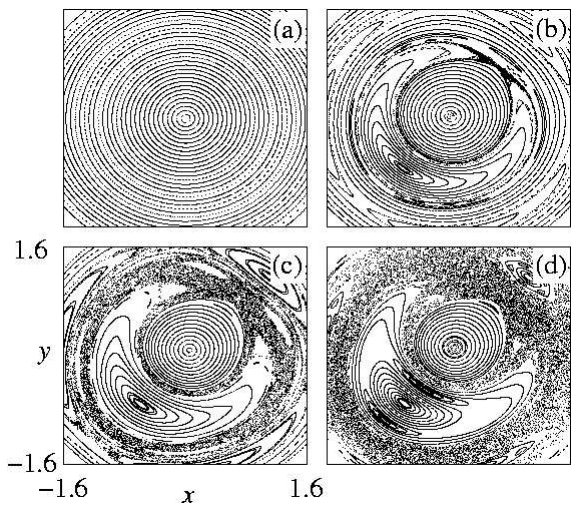


FIG. 1: Poincaré surface of section for the quantum trajectories generated by the wave function of Eq. (7) with  $b = c$  and  $a/b = 0$  (a), 0.0553 (b), 0.1138 (c) and 0.17651 (d) with fixed value of  $\gamma_1 = 3.876968$  and  $\gamma_2 = 2.684916$ . The trajectory of the vortex of the corresponding wave functions are shown in Fig. 2.

where  $\mathbf{w} \equiv \nabla\psi(\mathbf{r}_v(t))$  [10, 11]. We consider here 2-D systems but the generalization is straightforward.

Before presenting our analytical results we show a numerical simulation of quantum trajectories in a system consisting of a particle of unit mass in 2-D isotropic harmonic oscillator. We have set the angular frequency  $\omega = 1$ , so the Hamiltonian of the system results

$$H = -\frac{1}{2}\left(\frac{\partial^2}{\partial x^2} + \frac{\partial^2}{\partial y^2}\right) + \frac{1}{2}(x^2 + y^2). \quad (6)$$

Its eigenenergies are  $E_{n_x n_y} = n_x + n_y + 1$  and eigenfunctions  $\phi_{n_x n_y}(x, y) = \frac{\exp(-\frac{1}{2}(x^2 + y^2)) H_{n_x}(x) H_{n_y}(y)}{\sqrt{\pi} 2^{n_x+n_y} n_x! n_y!}$  with  $n_x = 0, 1, \dots$ ,  $n_y = 0, 1, \dots$  and  $H_n$  the  $n$ -th degree Hermite polynomial.

As initial state we choose a general combination of the first three eigenstates of the Hamiltonian of Eq. (6)

$$\psi_0 = a\phi_{00} + b\exp(-i\gamma_1)\phi_{10} + c\exp(-i\gamma_2)\phi_{01}, \quad (7)$$

with  $a, b, c, \gamma_1$  and  $\gamma_2$  real numbers and  $a^2 + b^2 + c^2 = 1$ , the normalization condition. A remarkable point is that this state generates a periodic time dependent velocity field with only one vortex. Moreover, the trajectory of the vortex  $\mathbf{r}_v(t)$  can be obtained analytically resulting  $(x_v(t), y_v(t)) = \left(\frac{a}{\sqrt{2}b} \frac{\sin(\gamma_2 - t)}{\sin(\gamma_1 - \gamma_2)}, \frac{a}{\sqrt{2}c} \frac{\sin(\gamma_1 - t)}{\sin(\gamma_1 - \gamma_2)}\right)$ . This fact allow us to see the influence of the movement of a vortex in the dynamics of the quantum trajectories without taking into account the possibility of instantaneous creation or annihilation of a vortex pair with opposite circulation [11, 12]. This important phenomenon will be studied elsewhere [13].

The non-autonomous velocity field generated by the wave function of Eq. (7) is periodic so the best surface of

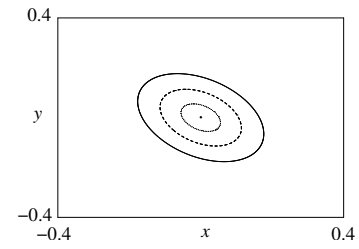


FIG. 2: Path described by the vortex of the velocity field generated by wave functions of Eq. (7) with  $b = c$  and  $a/b = 0$  (filled circle), 0.0553 (dotted line), 0.1138 (dashed line) and 0.17651 (solid line) with fixed value of  $\gamma_1 = 3.876968$  and  $\gamma_2 = 2.684916$ .

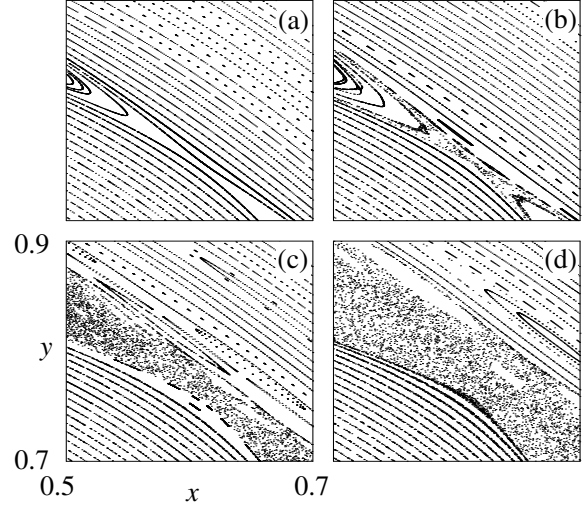


FIG. 3: Part of the Poincaré surface of section for the quantum trajectories generated by the wave function of Eq. (7) with small values of  $a/b$ . The parameter  $b = c$  and  $a/b = 0.01082$  (a), 0.02175 (b), 0.0328 (c) and 0.0440 (d) with fixed value of  $\gamma_1 = 3.876968$  and  $\gamma_2 = 2.684916$ .

section is given by fixing  $t = 2\pi n$  with  $n = 0, 1, \dots$  (also called a stroboscopic view). In Fig. 1 it is showed a surface of section with  $b = c$  and  $a/b = 0, 0.0553, 0.1138$  and  $0.17651$  with fixed value of  $\gamma_1 = 3.876968$  and  $\gamma_2 = 2.684916$ . The trajectory of the vortex for the cases studied in Fig. 1 is plotted in Fig. 2. It is clearly observed a transition to chaos as the parameter  $a/b$  is increased. If the position of vortex is fixed [see Fig. 1(a)] the trajectories are regular and no chaos is present. However, irregular dynamics is observed for small  $a/b$  [Fig. 1(b)]. The transition to irregular dynamics is showed in Fig. 3. The movement of the vortex produce a saddle point near  $(0.6, 0.75)$  and the stable and unstable manifold has a topological transverse intersection generating the well known homoclinic tangle [14].

Now we will show analytical results that explain the numerical experiments presented before. Our starting point is the following model: a particle of unit mass on the plane in the velocity field of Eq. (5) with the

stress that the trajectory of the vortex is a time periodic curve with period  $T_0$  and  $w_x = iw_y$  [15]. So, the non-autonomous vector field is equal to

$$\begin{aligned} v_x &= \frac{-(y - y_v(t))}{(x - x_v(t))^2 + (y - y_v(t))^2} \\ v_y &= \frac{(x - x_v(t))}{(x - x_v(t))^2 + (y - y_v(t))^2}. \end{aligned} \quad (8)$$

Taking  $\bar{x} = x - x_v(t)$   $\bar{y} = y - y_v(t)$  and writing in polar coordinates ( $\bar{x} = r \cos(\theta)$ ,  $\bar{y} = r \sin(\theta)$ ), the velocity field of Eq. (8) results

$$\begin{aligned} v_r &= r[\sin(\theta)y_v(t) + x_v(t) \cos(\theta)] \\ v_\theta &= \frac{1}{r} + \cos(\theta)y_v(t) - x_v(t) \sin(\theta). \end{aligned}$$

This non-autonomous velocity field can be seen as a perturbation of the autonomous velocity field  $\mathbf{v}_0 \equiv (0, \frac{1}{r})$  with  $\mathbf{G}_t(r, \theta) \equiv (r[\sin(\theta)y_v(t) + x_v(t) \cos(\theta)], \cos(\theta)y_v(t) - x_v(t) \sin(\theta))$  the time-periodic perturbation. Note that it is induced by the time dependent Hamiltonian

$$H(r, \theta, t) = \frac{1}{2} \log(r) + r[\cos(\theta)y_v(t) - \sin(\theta)x_v(t)]. \quad (9)$$

We consider periodic curves  $\mathbf{r}_v(t)$  such that

$$\int_0^{T_0} \cos(\theta)y_v(t) - x_v(t) \sin(\theta) dt ds \neq 0 \quad (10)$$

Under these hypothesis it is proved the following:

*there exists a saddle periodic point of the flow associated to the vector field of Eq. (8), exhibiting a homoclinic transversal intersection.*

This is the main result of the letter which implies that quantum trajectories show topological chaos. We illustrate here the geometrical arguments of the proof and we leave the full details for a future publication [16].

First, let us consider the flow  $\Phi_t^0$  associated to the autonomous velocity field  $\mathbf{v}_0$ . This flow is defined for every  $(x, y) \neq (0, 0)$ . So, given a positive time  $T_0$  follows that it is well defined the map  $R_0 = \Phi_{T_0}^0 : \mathbb{R}^2 \setminus \{(0, 0)\} \rightarrow \mathbb{R}^2 \setminus \{(0, 0)\}$ . The map  $R_0$  keeps invariant the set of points with same radius; i.e.: it keeps invariant the circles. Moreover, the circles are rotated with a rate of rotation inversely proportional to the radius [see Fig. 4(a) and (b)]. Observe that the map  $R_0$  resemble a twist map with the difference that in the present case, the rate of rotation grows to infinity when the radius is reduced. In other words, if the map  $R_0$  is written in polar coordinates, follows that  $R_0(r, \theta) = (r, \theta + \frac{1}{r}T_0)$ . We want to mention that for generic conservative perturbations of the twist

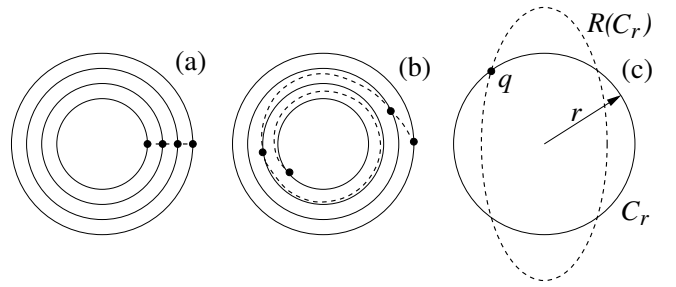


FIG. 4: (a) Schematic plot of the invariants of the non-perturbed map  $R_0$  generated by the autonomous velocity field  $\mathbf{v}_0$  (solid lines). With dashed line it is plotted a segment with  $\theta = 0$ . (b) Non-perturbed mapped  $R_0$  of the segment with  $\theta = 0$  (dashed line). (c) It is showed with dashed line the image of the perturbed map  $R$  of a circle  $C_r$  with radius  $r$  (solid line). A point  $q \in R(C_r) \cap C_r$  is also plotted.

map was proved in Ref. [17] the existence of homoclinic points associated to a saddle periodic point. This result is also extended for time periodic perturbation of a flow which exhibit an elliptic singularity [see Ref.[18]].

Assuming that the vortex moves periodically along a curve, the time dependent velocity field  $\mathbf{v}_t = \mathbf{v}_0 + \mathbf{G}_t$  induce a flow  $\Phi_t$  which is defined for every  $(x, y) \neq \{(0, 0)\}$ . So, it is well defined the map  $R = \Phi_{T_0} : \mathbb{R}^2 \setminus \{(0, 0)\} \rightarrow \mathbb{R}^2 \setminus \{(0, 0)\}$ . The flow  $\Phi_t$  is generated by a time periodic Hamiltonian [Eq. (9)], so  $R$  is a conservative map. From this property and using that the map can be extended continuously to  $(0,0)$  defining  $R(0,0) \equiv (0,0)$ , follows that the map  $R$  verify:

*Property A:* The map  $R$  also has the property that circles are rotated with a rate of rotation inversely proportional to the radius. In other words, if the map  $R$  is written in polar coordinates  $R(r, \theta) = (R^r(r, \theta), R^\theta(r, \theta))$ , then  $\partial_r R^\theta$  is of the the order of  $\frac{1}{r^2}$ .

*Property B:* The image of a small circles of radio  $r$  intersect transversally this circle; i.e:  $R(C_r) \cap C_r \neq \emptyset$  and if  $q \in R(C_r) \cap C_r$  then the tangent to  $R(C_r)$  in  $q$  and the tangent of  $C_r$  in  $q$  are not collinear [see Fig. 4(c)].

From *properties A* and *B* of the perturbed map  $R$  follows that for arbitrarily small  $r$  the map  $R$  has a fix point  $p_0$  with radius smaller than  $r$  and exhibiting a homoclinic transversal points. It is possible to show  $r$  does not have to be extremely small. This is done in two steps. First, we see that for each  $r$  we take a point  $(r, \theta_0(r))$  such that  $R^r(r, \theta_0(r)) = r$  which existences is guarantee by *property B*. Then, it is taken the angular coordinate  $\theta_1(r) = R^\theta(r, \theta_0(r))$ . From *property A* follows that the variation of  $\theta_1(r)$  is larger than the variation of  $\theta_0(r)$ ; in fact, the derivative of  $\theta_1(r)$  is of the order of  $\frac{1}{r^2}$ . Therefore, the graph of both functions has to intersects each other, which implies that there is  $r_0$  such that  $R(r_0, \theta_0(r_0)) = (r_0, \theta_0(r_0))$  [see Fig. 5 (a)].

To show that  $p_0$  has a transversal homoclinic point, first it is observed that the circle  $C_0$  of constant radius

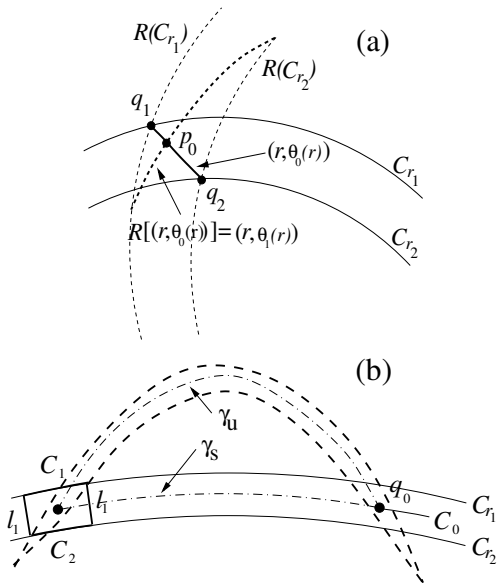


FIG. 5: Schematic plots to show the geometrical properties needed to prove the existence of a saddle periodic point with homoclinic transversal intersection. (a) It is represented with thick solid line the curve  $r \rightarrow (r, \theta_0(r))$ , and with thick dashed line the curve  $r \rightarrow R((r, \theta_0(r))) = (r, \theta_1(r))$  which intersect in the periodic point  $p_0$ . Two invariants circles ( $C_{r_1}$  and  $C_{r_2}$ ) and their perturbed mapping are also plotted. Note the transversal intersection between the circles and their respective mapping (points  $q_1$  and  $q_2$ ). (b) It is plotted with thick dashed line the mapping of the rectangle  $B$  (thick solid line) contained the periodic point  $p_0$ . With dash-dotted lines it is plotted the segments  $\gamma_u$  and  $\gamma_s$  that connects the periodic point  $p_0$  with the transversal intersection  $q_0$ . See text for more details.

that contains  $p_0$  and its image,  $R(C_0)$ , has at least two points of intersection (see Fig. 5 (b)). Let us denote  $q_0$  this other point of intersection of  $R(C_0)$  with  $C_0$ ; let us also take  $\gamma_u$  and  $\gamma_s$  the connected arc of  $R(C_0)$  and  $C_0$  respectively that contain  $p_0$  and  $q_0$ . Then, it is taken a rectangle  $B$  containing  $p_0$  and bounded by two pieces of arcs  $C_1$  and  $C_2$  contained in  $C_{r_1}$  and  $C_{r_2}$  respectively and two segments  $l_1$  and  $l_2$  contained in two different rays of constant angle. It is proved that  $B$  is contracted by  $R$  along directions closed to the tangent of the circles  $C_r$  and expanded along vectors closed to the tangent of  $R(C_r)$ . Moreover, it is proved the following: *i*)  $R(B)$  is closed to  $\gamma_u$  and intersects  $C_0$  in a point closed to  $q_0$ ; *ii*)  $R^{-1}(B)$  is closed to  $\gamma_s$  and intersects  $C_0$  in a point closed to  $q_0$ . The two previous items implies that the unstable manifold of  $p_0$  is closed to  $\gamma_u$  and the stable is closed to  $\gamma_s$ . In [19] it is possible to find similar argument to the case where the “vortex is in the infinite”. It is important to emphasize that, although we have been able to prove rigorously that motion of the vortex implies chaos in the model presented before, it seems that the former geometrical properties are fulfilled by the general velocity field [Eq. (5)] as was showed by the numerical experiments.

In summary, we have found an universal mechanism which leads that quantum trajectories have chaotic behavior. We show that the movement of vortices is a generic time dependent perturbation which creates a saddle point with a transversal homoclinic cross of their stable and unstable manifold. This transversal cross generates the well known Small horseshoe which is the origin of the complexity. Our results are of great importance due to the fact that such a deterministic orbits are an important theoretical tool for understanding and interpreting several quantum processes in different fields. On the other hand, our geometrical analysis of a singular velocity field could be useful for theoretical and applied problems of dynamical systems, as for example advection in non-stationary fluids [20].

This work received financial support from CONICET and UBACYT (X248).

- 
- [1] P. R. Holland. *The Quantum Theory of Motion* (Cambridge University Press, Cambridge, 1993).
  - [2] D. Dürr, S. Goldstein and N. Zanghì, *J. Stat. Phys.* **67**, 843 (1992).
  - [3] C. L. Loprore and R. E. Wyatt, *Phys. Rev. Lett.* **26**, 5190 (1999).
  - [4] O. V. Prezhdo and C. Brooksby, *Phys. Rev. Lett.* **86**, 3215 (2001).
  - [5] H. Wu and D. W. L. Sprung, *Phys. Lett. A* **196**, 229 (1994).
  - [6] Bohm D., *Phys. Rev.*, **85** (1952) 166; *ibid* **85** (1952) 194.
  - [7] Parmenter R. H. and Valentine R. W., *Phys. Lett. A*, **201** 1(1995); Frisk H., *Phys. Lett. A*, **227** 139 (1997); Konkel S. and Malowski A. J., *Phys. Lett. A*, **238** 95 (1998); J. A. Sales and J. Florencio, *Phys. Rev. E* **67** 016216 (2003).
  - [8] P. A. M. Dirac, *Proc. R. Soc. A* **133**, 60 (1931).
  - [9] I. Bialynicki-Birula and Z. Bialynicki-Birula, *Phys. Rev. D* **3**, 2410 (1971).
  - [10] P. Falsaperla and G. Fonte, *Phys. Lett. A*, **316** 382 (2003).
  - [11] I. Bialynicki-Birula, Z. Bialynicki-Birula and C. Sliwa, *Phys. Rev. A* **61**, 5190 (2000).
  - [12] J. O. Hirschfelder, *J. Chem. Phys.* **67** 5477, 1978.
  - [13] D.A.Wisniacki, F. Borondo and E. Pujals, unpublished.
  - [14] J. Palis and F. Takens, *Hyperbolicity and sensitive chaotic dynamics at homoclinic bifurcations* (Cambridge University Press, Cambridge, 1993).
  - [15] This is the simplest toy model because  $w_x$  and  $w_y$  are time dependent functions given by the derivatives of the wave function.
  - [16] E. Pujals and D. A. Wisniacki, unpublished.
  - [17] E. Zehnder. *Comm. Pure Appl. Math.* **26** 131 (1973).
  - [18] J. Guckenheimer and Ph. Holmes. *Nonlinear oscillations, dynamical systems, and bifurcations of vector fields.* (Springer-Verlag, New York, 1990).
  - [19] J. Moser, *Stable and random motions in dynamical systems: With special emphasis on celestial mechanics.* (Princeton University Press, Princeton, NJ, 2001).
  - [20] L. Kuznetsov and G. M. Zaslavsky, *Phys. Rev. E* **58**,

